

Statistical Analysis of Composite Spectra

A.Y. Abul-Magd,¹ H. L. Harney,² M.H. Simbel,¹ and H.A. Weidenmüller²

¹*Faculty of Science, Zagazig University, Zagazig, Egypt*

²*Max-Planck-Institut für Kernphysik, Heidelberg*

(Dated: June 27, 2018)

Abstract

We consider nearest-neighbor spacing distributions of composite ensembles of levels. These are obtained by combining independently unfolded sequences of levels containing only few levels each. Two problems arise in the spectral analysis of such data. One problem lies in fitting the nearest-neighbor spacing distribution to the histogram of level spacings obtained from the data. We show that the method of Bayesian inference is superior to this procedure. The second problem occurs when one unfolds such short sequences. We show that the unfolding procedure generically leads to an overestimate of the chaoticity parameter. This trend is absent in the presence of long-range level correlations. Thus, composite ensembles of levels from a system with long-range spectral stiffness yield reliable information about the chaotic behavior of the system.

PACS numbers: 05.45.Mt, 02.50.Tt, 24.60.Lz

I. INTRODUCTION

The statistical analysis of spectra aims at a comparison of the spectral fluctuation properties of a given physical system with theoretical predictions like those of random–matrix theory (RMT), those for integrable systems, or interpolations between these two limiting cases.

Specific problems arise whenever the spectra under consideration involve a relatively small number of levels. This is the situation in the analysis of spectra of nuclei in the ground–state domain [1, 2, 3, 4, 5, 6, 7, 8, 9], of atomic spectra [10, 11, 12], and of molecular spectra [13, 14, 15]. Here, one usually deals with sequences of levels of the same spin and parity containing only 5 or 10 levels. Several or many such sequences are then combined to obtain an ensemble of statistically relevant size. The sequences forming the ensemble may involve levels of different spin–parity and/or levels from different nuclei. The resulting data set is typically analysed with regard to the nearest–neighbor spacing (NNS) distribution only. In view of the shortness of the individual sequences, correlations between spacings of levels are not investigated.

In the present paper, we address two problems which arise in the analysis of such data. First, we ask whether a fit to a histogram of the NNS distribution is the optimal way to analyze the data. We compare this method with the method of Bayesian inference which has been successfully used to analyze the statistical properties of coupled microwave resonators [16, 17]. Second, for a reliable analysis, one has to ”unfold” the individual sequences. This yields a new data set with mean level spacing unity. Then, one combines these level sequences to form a larger ensemble of spacings suitable for the statistical analysis. How big is the statistical error due to this unfolding procedure? We answer this question for two extreme cases where the spacings are taken from a spectrum without (with) the long–range rigidity typical for chaotic systems, respectively.

In Section II, we give a brief summary of the NNS distribution and of spectral analyses using it. In Section III, we give a short account of Bayesian inference tailored to the problems just mentioned. In Section IV, we address the above–mentioned two problems. Section V contains a summary and our conclusions.

II. THE NNS DISTRIBUTION

The canonical ensembles of random-matrix theory (RMT) [18] are classified according to their symmetries. Here, we focus attention on systems which are invariant under time reversal and under space rotations. Such systems are represented by the Gaussian orthogonal ensemble (GOE) of random matrices. The NNS distribution of levels of the GOE is well approximated by Wigner's surmise [19]

$$p_W(s) = \frac{\pi}{2} s \exp\left(-\frac{\pi}{4} s^2\right). \quad (1)$$

Here, s is the spacing of neighboring levels in units of the mean level spacing.

RMT was introduced originally to describe the spectral fluctuation properties of complex quantum systems. Later, it has been conjectured [20] that RMT also applies to quantum systems whose classical counterpart is chaotic. This conjecture has enormously widened the range of applications of RMT [21, 22] and has led to a juxtaposition of RMT and of the theoretical description of quantum systems which are integrable in the classical limit. The latter possess a NNS distribution which is generically given by the Poisson distribution,

$$p_P(s) = \exp(-s). \quad (2)$$

There also exist intermediate situations. Examples are (i) mixed systems where the motion in some parts of classical phase space is regular and in other parts, chaotic, see Refs. [21, 23, 24, 25] and references therein; (ii) pseudointegrable systems which possess singularities and are integrable in the absence of these singularities, see e.g. Refs. [26, 27, 28]; (iii) fully chaotic systems where a conserved symmetry is dynamically broken, or is ignored.

Here we focus attention on case (iii). The Hamiltonian for a system with strictly conserved symmetry is block-diagonal. Each block is characterized by a quantum number (or a set of quantum numbers) of the symmetry under consideration and may be separately considered as a member of a GOE. Symmetry breaking is modelled by introducing off-diagonal blocks that couple diagonal blocks with different quantum numbers. The resulting spectrum differs from GOE predictions. Such modelling has been useful in the following cases. (i) Isospin mixing in nuclear spectra and reactions [29]. (ii) Isospin mixing in the low-lying states of ^{26}Al [5]. (iii) The gradual breaking of a point-group symmetry (which is statistically fully equivalent to the

breaking of a quantum number like isospin) in an experiment with monocrystalline quartz blocks [30]. (iv) The electromagnetic coupling of the resonances in two superconducting microwave resonators [31]. The statistical analyses relating to some of these cases can be found in Refs. [1, 2, 3, 4, 5, 6, 7, 8, 9] and [16, 17, 32]. Ignoring a conserved symmetry leads to a superposition of several GOE spectra and to spectral fluctuation properties which are similar to those of the cases considered above. Very strong mixing of states possessing different symmetries leads to a GOE distribution, and the superposition of many GOE spectra leads to a NNS distribution which is Poissonian.

Thus, there is a variety of physical situations that give rise to level fluctuations which are intermediate between the GOE and the Poisson cases. We attempt to describe the NNS distribution in all these intermediate situations by a one-parameter family of functions interpolating between expressions (1) and (2). This family is defined in Section III A. We are aware of the fact that our procedure cannot be exact. Arguments will be given to justify its use but it remains an approximation.

III. BAYESIAN ANALYSIS OF NNS DISTRIBUTIONS

The Bayesian analysis of the NNS distribution proceeds in three steps. (i) We propose a probability distribution $p(s, f)$ for the observed spacings s of nearest neighbors. This function depends parametrically upon the parameter f which measures the deviation from GOE statistics. It is our aim to determine f from the data. (ii) We determine the posterior distribution $P(f|s)$ for the parameter f . (iii) We deduce the optimum value of f together with its statistical error. The three steps are outlined in the three subsections which follow.

A. Proposed NNS distribution

To construct $p(s, f)$, we consider a spectrum S containing levels of the same spin and parity. (In practice, we usually deal with a set of spectra but consider only a single one in the present Section. The generalisation to a set of spectra is considered in Section IV B). The levels in S may, however, differ in other conserved quantum numbers which are either unknown or ignored. The spectrum S can then be broken up into m sub-spectra S_j of independent sequences of levels, with $j = 1, \dots, m$. The fractional level number of S_j is

denoted by f_j where $0 < f_j \leq 1$ and $\sum_{j=1}^m f_j = 1$. Let $p_j(s)$, $j = 1 \dots m$, denote the NNS distribution for the sub-spectrum S_j . We assume that each of the distributions $p_j(s)$ is given by the GOE and has unit mean level spacing. To an excellent approximation, the p_j 's are then given by Wigner's surmise (1).

The construction of the NNS distribution $p(s, f_1, \dots, f_{m-1})$ for the superposition spectrum S (with unit mean level spacing) from the $p_j(s)$'s was explicitly carried out by Rosenzweig and Porter [10]. Their construction is not useful in the present context because in practice, we do not know the number m of sub-spectra, nor is it possible to determine all the parameters f_j from the data. To overcome this difficulty, we use an approximation scheme first proposed in Ref. [33] which leads to an approximate NNS distribution for S , viz.

$$p(s, f) = \left[1 - f + f (0.7 + 0.3f) \frac{\pi s}{2} \right] \times \exp \left\{ - (1 - f) s - f (0.7 + 0.3f) \frac{\pi s^2}{4} \right\}. \quad (3)$$

This function depends on only a single parameter, the mean fractional level number $f = \sum_{j=1}^m f_j^2$ for the superimposed subspectra. This quantity will eventually be used as a fit parameter. The derivation of Eq. (3) and the definition of f are discussed in Appendix A.

For a large number m of sub-spectra, f is of the order of $1/m$ and, thus, small. In this limit, $p(s, f)$ approaches $p(s, 0) = p_P(s)$ given by Eq. (2). This expresses the well-known fact that the superposition of many GOE level sequences produces a Poissonian sequence. On the other hand, when $f \rightarrow 1$, $p(s, f)$ approaches the NNS of the GOE. This is why we refer to f as to the chaoticity parameter. We use $p(s, f)$ as defined above for the analysis of the data.

Our model for $p(s, f)$ has been constructed with case (iii) of Section II in mind, even when the symmetries are only weakly broken. In that case, the distribution (3) is not accurate for very small spacings because $p(s, f)$ differs from zero at $s = 0$ while the symmetry-breaking interaction lifts all degeneracies. However, this defect should not affect the spacing distribution beyond the domain of very small spacings. The magnitude of this domain depends on the ratio of the strength of the symmetry-breaking interaction to the mean level spacing.

For the other cases of intermediate situations mentioned in Section II, our model may not be the best choice. The experimental NNS distributions of mixed systems (case (i)) are frequently analyzed using Brody's interpolation formula [34], $p(s) = a(\gamma + 1)s^\gamma \exp(-as^{\gamma+1})$,

where γ is a fit parameter and $a = \left[\Gamma \left(\frac{\gamma+2}{\gamma+1} \right) \right]^{\gamma+1}$, although Eq. (3) often also provides a reasonable representation, see Refs. [6, 24, 33]. Case (ii) (pseudointegrable systems) cannot be described in the framework of the present model. These systems are successfully described by the so-called semi-Poisson statistics [35] where the NNS distribution is $p(s) = 2s \exp(-4s)$.

B. Posterior Distribution

We turn to the second step of Bayesian inference, the calculation of the posterior distribution $P(f|\mathbf{s})$ for f given a set $\mathbf{s} = (s_1, s_2, \dots, s_N)$ of N spacings s_j with $j = 1, \dots, N$. We take the experimental s_j to be statistically independent. This assumption does not apply in general. Indeed, the GOE produces significant correlations between subsequent spacings. However, the correlations become small for spacings that are separated by a few levels. Under this assumption, the conditional probability distribution $p(\mathbf{s}|f)$ of the set of spacings \mathbf{s} is given by

$$p(\mathbf{s}|f) = \prod_{i=1}^N p(s_i, f), \quad (4)$$

with $p(s_i, f)$ given by Eq. (3). Bayes' theorem then provides the posterior distribution

$$P(f|\mathbf{s}) = \frac{p(\mathbf{s}|f)\mu(f)}{M(\mathbf{s})} \quad (5)$$

of the parameter f given the events \mathbf{s} . Here, $\mu(f)$ is the prior distribution and

$$M(\mathbf{s}) = \int_0^1 p(\mathbf{s}|f) \mu(f) df \quad (6)$$

is the normalization.

To find the prior distribution, we use Jeffreys' rule [36] discussed in Chap. 9 of Ref. [38],

$$\mu(f) \propto \left| \int p(\mathbf{s}|f) [\partial \ln p(\mathbf{s}|f) / \partial f]^2 ds \right|^{1/2}. \quad (7)$$

This formula — suggested 60 years ago — has been justified later through a combination of arguments based on symmetry and differential geometry [37, 38]. The prior distribution may be intuitively interpreted as the distribution ascribed to f in the absence of any observed s . However, this interpretation requires additional arguments when μ is an improper distribution. A mathematically more satisfactory interpretation of μ considers μ as the measure in the space of f . This interpretation justifies Jeffreys' rule as that rule yields the invariant measure of a suitable symmetry group.

Details on the posterior distribution can be found in Appendix B.

C. Best-fit value for f

The third and last step of the Bayesian analysis consists in determining the best-fit value and the associated error of the chaoticity parameter f for each NNS distribution. When $P(f|\mathbf{s})$ is not Gaussian, the best-fit value of f cannot be taken as the most probable value. Rather we take the best-fit value to be the mean value \bar{f} and measure the error by the standard deviation σ of the posterior distribution (B7), i.e.

$$\bar{f} = \int_0^1 f P(f|\mathbf{s}) df \quad \text{and} \quad \sigma^2 = \int_0^1 (f - \bar{f})^2 P(f|\mathbf{s}) df. \quad (8)$$

The second equation (8) does not provide the optimal definition of an error interval, see Chap. 3 of [38], but a useful approximation.

IV. ANALYSIS OF COMPOSITE ENSEMBLES

In the present Section we address the unfolding procedure for a large number of short sequences of level spacings. We do so for two cases: We study short sequences of levels that do not (do) possess the rigidity of GOE spectra. This is done in Subsections IV A (IV B, respectively). We show that unfolding leads to an overestimation of the chaoticity parameter in the first but not in the second case. Thus, long-range order is important for a reliable unfolding. In Subsection (IV C) we comment on this point.

A. The surrogate ensemble

Short sequences that lack GOE rigidity are taken from what we call the surrogate ensemble, a set of statistically independent spacings obtained with the help of a random-number generator. With this ensemble we also test (in Section IV A 2) the method of statistical analysis defined in Section III.

1. The uniform surrogate ensemble

To obtain the uniform surrogate ensembles, we generate a set of random numbers r_j , $j = 1 \dots l$, from a distribution with unit density between 0 and 1. We equate the cumulative spacing distribution W of Eq. (A7) (with q and Q given by Eqs. (A10) and (A15),

Spectrum	Analysis method	$N = 50$	$N = 100$	$N = 200$
Uniform surrogate ensemble	0.2-bin histogram	0.90 ± 0.12	0.75 ± 0.11	0.71 ± 0.06
	0.3-bin histogram	0.90 ± 0.14	0.80 ± 0.11	0.72 ± 0.06
	Bayesian	0.67 ± 0.14	0.61 ± 0.13	0.63 ± 0.07

TABLE I: Bayesian method vs. chi-squared fit

respectively) with each of these random numbers. The associated spacing s_j is then obtained by solving Eq. (A7) for s . Setting the chaoticity parameter to $f_t = 0.60$, one obtains

$$s_i = -0.482 + \sqrt{0.233 - 2.41 \ln(1 - r_i)}. \quad (9)$$

In this way we generate three surrogate ensembles of 50, 100, and 200 spacings, respectively.

In each ensemble these spacings are statistically independent, have mean spacing unity, and follow the distribution Eq. (3). The expression “uniform ensemble” refers to the uniform statistical properties of the spacings. A spectrum constructed from a sequence of such spacings lacks the rigidity of GOE spectra.

The value f_t is referred to as the “true” value of f . It is checked in Section IV A 2 below whether a statistical analysis of short sequences of spacings does reproduce this value.

2. Comparison of two statistical inferences

We use the three surrogate ensembles to compare two methods of statistical inference: (i) We fit the conditional distribution (3) to a histogram of the spacings and (ii) we use the Bayesian method.

(i) The bin size for the histograms was taken once equal to 0.2 and once equal to 0.3. We determine the chaoticity parameter f for each of the six histograms by a chi-squared fit to the NNS distribution (3). The results are given in Figs. 1 and 2 and in Tab. I.

The Figures show that the shapes of the histograms do not exactly follow the distribution (3), especially for the smallest ensemble. Increasing the bin size of the histograms leads to shapes that better agree with the analytical distribution. One sees this by comparing Figs. 1 and 2. The chi-squared fit yields values for f that differ from the true value 0.60, and the difference is statistically significant, particularly for the large ensemble. This observation suggests that one should not analyze a small sample of data by a fit to a histogram.

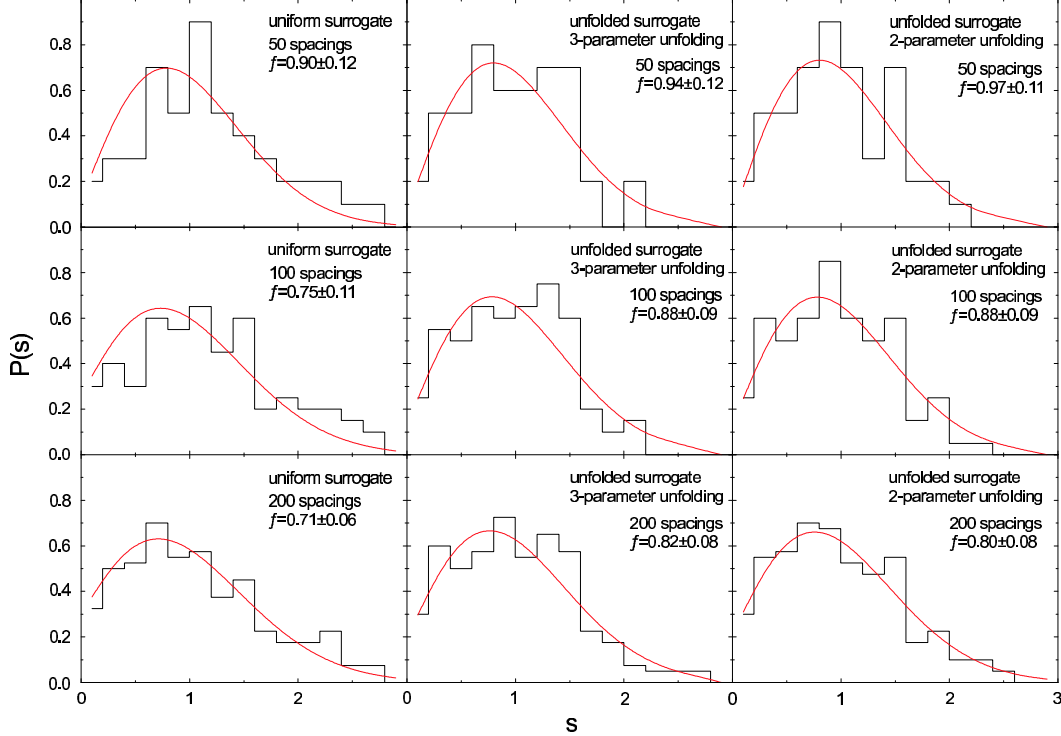


FIG. 1: Bayesian inference compared to chi-squared fits of the distribution (3) to the histograms of the surrogate ensemble. The first column of graphs presents uniform surrogate ensembles. The second and third columns present unfolded surrogate ensembles. The bin size is $\Delta s = 0.2$.

The reason is discussed in Chap. 16 of Ref. [38]: The chi-squared fit to a histogram is an approximation to the Bayesian procedure requiring that the number of counts in each bin is large.

(ii) The Bayesian method does not require any binning of the data. The posterior distribution (5) is written in terms of the prior $\mu(f)$ and a function $\phi(f)$ as

$$P(f|\mathbf{s}) \propto \mu(f) \exp(-N\phi(f)) \quad (10)$$

for the three uniform surrogate ensembles. We take the prior μ from the approximation (B1) in Appendix B. The exponent $\phi(f)$ is approximated by the cubic form in Eq. (B5). The quality of this approximation is demonstrated in Sec. IV B 2. In the three cases, we determine \bar{f} and the variance σ^2 of Sec. III C. The results are given in Tab. I in the form of $\bar{f} \pm \sigma$. We find that the Bayesian method correctly reproduces the true value of $f_t = 0.60$ within the statistical error — for all three distributions involving 50, 100, and 200

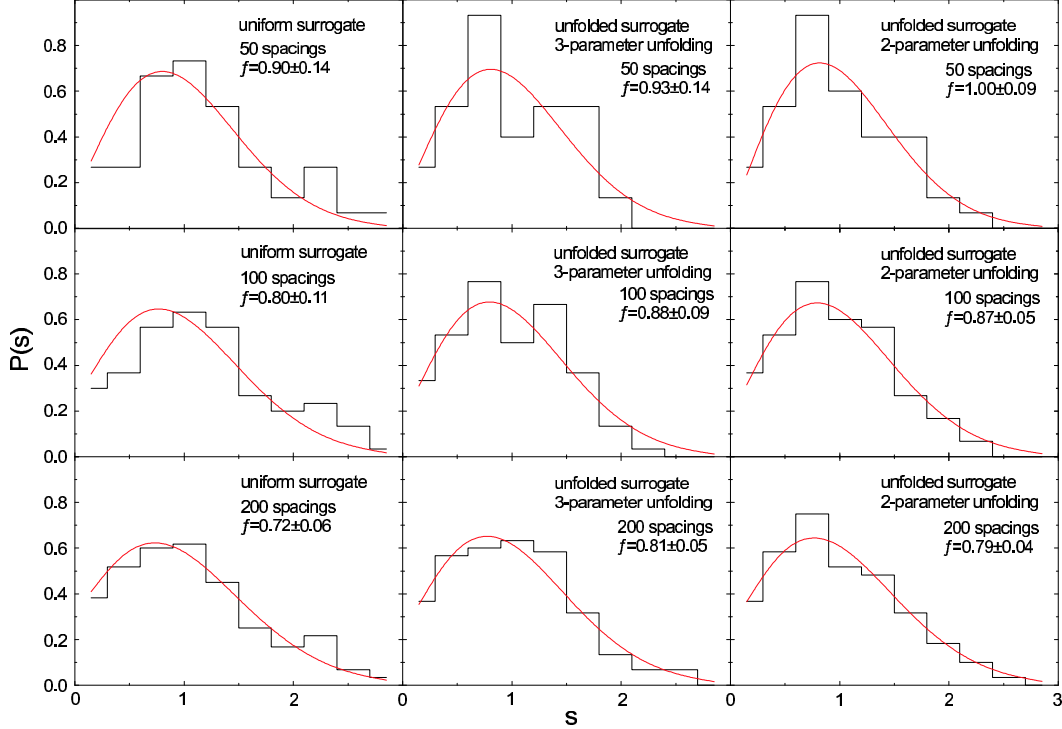


FIG. 2: Fig. 2. The same as on Fig. 1 except for the bin size $\Delta s = 0.3$.

spacings. This indicates that the value of \bar{f} is a reliable estimate of the true value f_t . Tab. I contains the cases where the discrepancy is especially large. However, the very appearance of a discrepancy and the fact that the chi-squared fit – when applied to Poisson statistics – is less well founded, show that for small samples of level spacings the Bayesian method is superior to the fitting of a histogram. Therefore, in the present article we henceforth report only results obtained with the Bayesian method (although we have also obtained in parallel the chi-squared fits).

3. Impact of the unfolding procedure

Experimental spectra do not possess constant average level density. Rather the average level density increases with increasing excitation energy. “Unfolding” is the procedure that transforms such a spectrum into one with constant average level density. In the case of a single long spectrum unfolding is a standard procedure: It consists in fitting a slowly varying function $\epsilon(E, \alpha)$ to the experimental staircase function $N(E)$ of the integrated level density

(a function of energy E). Examples of functions ϵ are given in Eqs. (12,13) below. The fit is obtained by optimizing a set of parameters α . The function ϵ depends monotonically on E . Therefore, one can transform E to ϵ . With respect to the new energy variable ϵ , the level density is equal to unity.

Here we consider an ensemble of spacings given by many short sequences. For such a "composite ensemble", unfolding is not a standard procedure. One may argue that for composite ensembles, unfolding is altogether irrelevant because the mean level density changes slowly. However, sequences of levels of the same spin and parity taken from the nuclear ground-state domain are examples to the contrary.

To test the impact of the unfolding procedure, we generate short sequences of levels from the three uniform surrogate ensembles by arranging the spacings in some order. Each such sequence is then artificially folded with a monotonically increasing function of energy. An unfolding procedure is subsequently applied to each sequence. The unfolding procedure does not trivially reproduce the initial sequences and yields the "unfolded surrogate" ensembles. Finally, the chaoticity parameter f is determined.

From the surrogate ensemble containing 50 spacings, we constructed 8 level sequences. There are 3 sequences of 5 levels, 2 sequences of 6 levels, and one sequence each of 9, of 10 and of 12 levels. The ensemble containing 100 spacings was arranged into 6 sequences of 5 levels, 4 sequences of 6 levels, two sequences of 7 and two sequences of 10 levels, and one sequence each of 8, 9, and 12 levels. From the ensemble containing 200 spacings, we constructed 9 sequences of 5 levels, 6 sequences of 6 levels, 5 sequences of 7 levels, 3 sequences of 8 levels, 4 sequences of 10 levels, and one sequence each of 9, 17, and 24 levels. Our choices mirror typical sets of empirical data in nuclei. We interpret the spacing sequences as level sequences and identify in each sequence the ground state E_0 and the excited states E_i . We then construct "intermediate" level sequences $\{E'_i\}$ by the transformation

$$E'_i = aE_i^b \quad i = 0, \dots, i_{\max} \quad (11)$$

where i_{\max} denotes the number of spacings in the sequence, and where a and b are positive constants. We refer to the transition from the energy scale E to the scale E' as to the "folding" of the spectrum.

To make the test as realistic as possible, we determined the parameters a and b by fitting the excitation energies of the 2^+ levels of thirty nuclei to Eq. (11). We averaged the power

Spectrum	Analysis method	$N = 50$	$N = 100$	$N = 200$
Uniform surrogate ensemble	Bayesian	0.67 ± 0.14	0.61 ± 0.13	0.63 ± 0.07
2-parameter unfolding	Bayesian	0.88 ± 0.10	0.83 ± 0.08	0.77 ± 0.06
3-parameter unfolding	Bayesian	0.91 ± 0.08	0.86 ± 0.08	0.78 ± 0.06

TABLE II: Impact of the unfolding procedure on the surrogate ensembles

b over the thirty cases. We then determined the values of a that reproduced the positions of the highest 2^+ level under consideration in each nucleus, and took the average of a . This procedure yielded $a = 0.36$ and $b = 2.82$. These values were used to generate the folded spectra.

The intermediate sequences obtained in this manner are unfolded with the constant-temperature formula [2]

$$\epsilon(E') = \epsilon_0 + \exp\left(\frac{E' - E_0}{T}\right) \quad (12)$$

for the cumulative level density. (In the case of experimentally given sequences, the energy dependence of the mean level density is not known a priori. To simulate this situation we chose that dependence to be different in Eqs. (11) and (12)). The unfolding was done in two versions. In a three-parameter version, one searches for the parameters $\alpha = (\epsilon_0, E_0, T)$ in Eq. (12); in a two-parameter version, one uses the simpler expression

$$\epsilon(E') = N_1 \exp\left(\frac{E'}{T_1}\right) \quad (13)$$

and searches for $\alpha = (N_1, T_1)$. Combining the results in each case, we obtained the three “unfolded surrogate” ensembles of 50, 100, and 200 spacings, respectively, and applied Bayesian statistics.

The results of this procedure are given in Tab. IV A 3. We see that the inferred chaoticity parameter is significantly larger than the true value $f_t = 0.60$. The ensemble containing 50 spacings appears to be almost chaotic after unfolding! We explain this as follows.

Unfolding small sequences yields spacings closer to the mean value (unity) than would be the case for larger sequences. This is seen by considering the extreme case of sequences where the number of levels in each sequence equals the number of parameters α . Here, unfolding would yield a picked-fence spectrum without any fluctuations of the NNS. Thus, the number of spacings in each sequence must obviously be larger than the number of parameters used

in unfolding. Still, for small sequences unfolding introduces a bias away from Poisson and towards the GOE, i.e., the value of f is found larger than the true one.

To show that our argument applies, we created another unfolded surrogate ensemble with 50 spacings from only 3 sequences. One of these sequences is composed of 12 levels, one of 17 levels, and one of 24 levels. The two-parameter unfolding yielded $\bar{f} = 0.74 \pm 0.13$. This is in better agreement with the true value than the result $\bar{f} = 0.88 \pm 0.10$ from the 14-sequence ensemble given in Tab. IV A 3. Correspondingly, the three-parameter unfolding yielded $\bar{f} = 0.73 \pm 0.13$ instead of $\bar{f} = 0.91 \pm 0.08$ in Tab. IV A 3.

The values of \bar{f} obtained in Tab. IV A 3 from the unfolded surrogate ensembles decrease as the number of spacings increases although they remain different from the true value of $f_t = 0.60$, even in the case of 200 spacings.

B. The GOE ensemble

We now introduce a composite ensemble of short sequences of levels following GOE statistics and investigate the effect of unfolding for this ensemble. GOE spectra differ from those obtained from the surrogate ensembles by their spectral rigidity. We shall see that the rigidity is important for unfolding.

When one adds N independent random spacings (as is done in the case of the surrogate ensembles), the expectation value \bar{L} of the length of the spectrum is $\bar{L} = ND$, where D is the mean spacing, while the variance of L behaves as $\text{var}(L) = \bar{L}^2 - \bar{L}^2 \propto N$, so that

$$\sqrt{\text{var}(L)/\bar{L}} \propto N^{-1/2}. \quad (14)$$

In contradistinction, when one takes N consecutive levels out of a GOE spectrum, the relative r.m.s. deviation of the length L of that sequence is

$$\sqrt{\text{var}(L)/\bar{L}} \propto (\ln N)^{1/2}/N. \quad (15)$$

This makes a noticeable difference particularly for small N .

1. The uniform composite GOE ensemble

The uniform composite GOE ensemble is constructed by using the results of the experiment by Alt *et al.* [31]. These authors measured the resonance spectra of a pair of

electromagnetically coupled superconducting microwave resonators each having the shape of a quarter of a Bunimovich stadium billiard. The complete spectra of the two stadia contain 608 and 883 resonances, respectively. We consider the case where the resonators are uncoupled. Then the measured spectrum is a superposition of two independent GOE spectra. It has been unfolded as a whole by Alt *et al.* [31]. The resulting spectrum was uniform and the spacing distribution was well described by Eq. (3) with the true value $f_t = 0.52$, see Ref. [17]. We ignored the low-energy part of the complete spectrum and used levels No. 59–463 to generate three “uniform GOE ensembles” of 50, 100, and 200 spacings, respectively. The composition of these ensembles is exactly the same as in Section IV A 3: The 50-spacing ensemble, for instance, consists of 8 sequences of (consecutive) levels with 3 sequences of 5 levels, 2 sequences of 6 levels, one sequence of 9, 10, 12 levels, respectively, etc. Care was taken to separate each sequence from the next by a gap of at least 5 levels in the original spectrum of Ref. [31]. This was done in order to reduce or even remove the correlations between levels belonging to different sequences: The long-range order of GOE spectra does not imply strong correlations between spacings that are separated by a few levels in the original spectrum.

The construction just described corresponds to case (iii) of Section II: The sequences are taken from a chaotic quantum system with an ignored symmetry. We refer to the result as to the “uniform composite GOE ensemble” because the sequences contained in it uniformly possess GOE statistics with average level spacing unity. We first convince ourselves that f can be correctly inferred from this ensemble (Section IV B 2). In a second step, the sequences are folded and again unfolded. This produces the “unfolded composite GOE ensemble”. We expect that this ensemble represents typical experimental situations. We determine the influence of the unfolding procedure on f by comparing the result with the true value f_t .

2. Analysis of the uniform composite GOE ensemble

To determine the chaoticity parameter f for the three uniform composite GOE ensembles, we have expressed the posterior distribution (5) by the function $\phi(f)$ via Eq. (10) as in Section IV A 2. Again $\phi(f)$ was approximated by the cubic form Eq. (B5). The quality of this approximation is demonstrated in Fig. 3. A similar picture holds for the cases treated in Section IV A 2. We determined \bar{f} and the variance σ^2 , see Section III C. The results are

Spectrum	Analysis method	$N = 50$	$N = 100$	$N = 200$
Uniform GOE	Bayesian	0.56 ± 0.14	0.52 ± 0.10	0.55 ± 0.07
2-parameter unfolding	Bayesian	0.59 ± 0.14	0.56 ± 0.09	0.58 ± 0.09
3-parameter unfolding	Bayesian	0.62 ± 0.13	0.58 ± 0.09	0.62 ± 0.06

TABLE III: Impact of the unfolding procedure on the GOE ensembles

given in Tab. III under the label “uniform GOE ensemble” in the form $\bar{f} \pm \sigma$. We find the true value $f_t = 0.52$ for all three uniform GOE ensembles involving 50, 100, and 200 spacings.

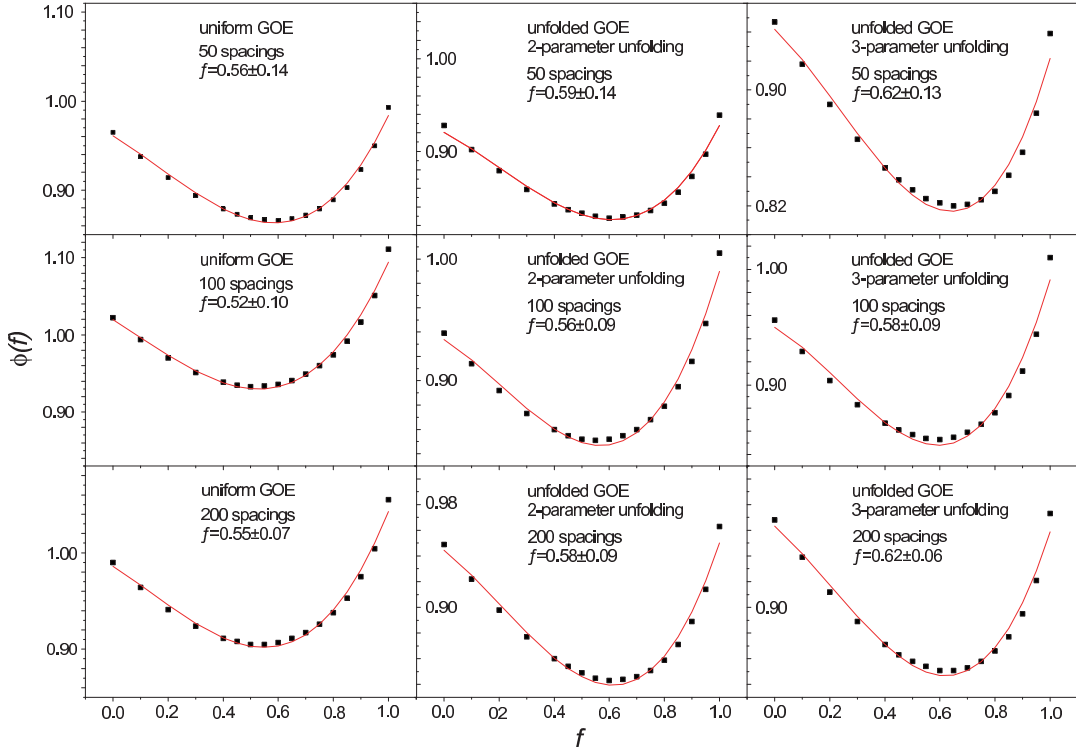


FIG. 3: The posterior distribution (10) in the approximation (B5).

GOE spacings are correlated, especially those that closely follow each other in a given sequence. Using Eq. (4), we have neglected these correlations. Our results indicate that such correlations are immaterial for the determination of f .

3. Impact of the unfolding procedure

We determine the impact of unfolding the sequences in the GOE ensemble. Let $\{E_i\}$ be a sequence of levels taken from the uniform composite GOE ensemble. We construct an intermediate sequence $\{E'_i\}$ by folding $\{E_i\}$ with the function of Eq. (11). The parameters a and b are as in Section IV A 3. The intermediate sequence is unfolded with the help of formula (12) (for 3-parameter unfolding) or (13) (for 2-parameter unfolding). This yields an unfolded sequence $\{\epsilon_i\}$. The “unfolded composite GOE ensemble” is composed of all unfolded sequences. From the unfolded composite GOE ensembles, the chaoticity parameter f is inferred. The results are given in Tab. III. We conclude the following:

(i) Inferring f after 2-parameter or 3-parameter unfolding produces statistically indistinguishable results. This confirms the insensitivity of the final ensemble of spacings to the form of the unfolding function, a hypothesis which has always been implicitly made in previous analyses. It is indeed a condition for the validity of the statistical analysis of spectral fluctuations. We do not investigate this point further because the insensitivity is known from previous studies.

(ii) In the unfolded GOE ensembles, the true value of f is correctly inferred (within the error given by the analysis). It seems that the rigidity of the spectrum of the uniform GOE ensemble guarantees that the unfolding procedure only weakly alters the fluctuation properties of the NNS. In the next subsection, we offer an explanation for this somewhat surprising fact.

C. A better way to infer f

In our analysis, we have separated the unfolding procedure (which was done first) from the procedure of inferring f . However, unfolding a sequence of levels amounts to inferring the parameters α of Eqs. (12) and (13) by way of a fit. The fit does not determine the value of α precisely. Rather, it is itself a procedure of statistical inference and — speaking in terms of Bayesian statistics — it produces a distribution of α . We have disregarded this fact. Instead we have used the best-fit-value of α in the subsequent estimate of f .

A more satisfactory procedure would be the following: One starts from the distribution $p(\mathbf{s}|f, \alpha)$ of the spacings \mathbf{s} conditioned by the chaoticity parameter f and the parameters

α for all the sequences contained in the composite ensemble (surrogate or GOE). Hence, p now is the distribution of the raw data before applying any transformation. The posterior distribution of f is determined after integration over the α . In this way one would not consider α as given; rather one would infer f after projecting the distribution of all unknown parameters unto the subspace of the interesting one. In fact, the integration over the uninteresting parameters is somewhat more complicated because it touches the question of a possible “marginalisation paradox”. Details are discussed in Chap. 12 of [38].

At any rate, one expects that f is determined with smaller error when α is given than when α is integrated over. For the example of a simple Gaussian model this is demonstrated in Appendix C.

We have not performed the integration over the uninteresting parameters α . To the best of our knowledge nobody has taken such a course so far. This is probably because the method would require a considerable effort — especially for a composite ensemble where α is high-dimensional. We conjecture that the integration over α would yield error intervals for f that would cover the true value in both cases, the case of the surrogate ensemble and the case of the GOE ensemble.

This would mean that in the case of the GOE ensemble and under the simplifying assumption that α is known, we have found reasonable error intervals. In the case of the surrogate ensemble, our simplification seems to fail and we have obtained incorrect (i.e., too small) error intervals. Our hypothesis can be made plausible by comparing two spectra containing the same number of levels. One of the spectra displays long-range stiffness, the other, local clustering of levels. The first spectrum allows for a clearer separation between fluctuations and secular variations than the second one because local clustering may be confused with a secular variation. The fitting procedure would react to this difference and in the first case ascribe a smaller error to α than in the second case.

V. SUMMARY AND CONCLUSIONS

In the present paper we have tested the reliability of a statistical analysis of spectral information contained in many short sequences of levels. We have used three uniform surrogate ensembles with known chaoticity parameter $f = f_t$ containing 50, 100 and 200 spacings, respectively. The surrogate ensembles are due to a random-number generator, with spac-

ings that are free of the rigidity of chaotic quantum spectra. The GOE ensembles were constructed from one long experimental spectrum with chaotic quantum behaviour, unit mean level spacing, and known chaoticity parameter f_t . The spectrum was cut into short sequences. The sequences were made statistically independent by disregarding a sufficient number of levels between them. We constructed three uniform composite GOE ensembles with 50, 100, and 200 spacings, respectively. (We believe that these ensembles simulate usual experimental cases). In both cases (the surrogate ensembles and the GOE ensembles), the method of Bayesian inference reproduces the true value f_t within the relevant error.

We have investigated the reliability of the unfolding procedure for composite ensembles of levels consisting of many short sequences. This was done by folding sequences of levels constructed from both, the uniform ensembles and the GOE ensembles, with a monotonically increasing function of energy. The resulting sequences were then unfolded with the help of a different unfolding function. The NNS distributions obtained in this way were combined to form unfolded ensembles. The resulting chaoticity parameters were determined and compared to the known true value f_t .

The chaoticity parameter f inferred from the unfolded surrogate ensembles is too large by about 15% for the ensembles containing 50 and 100 spacings, and by about 7% for the one containing 200 spacings. These discrepancies are statistically significant. We have shown that the overestimate is due to the occurrence of many sequences containing a small number of levels each and would be alleviated if a few long sequences were available instead. Generically, however, unfolded surrogate ensembles provide a bias towards full chaoticity. This is not the case for the GOE ensembles where the true value f_t is correctly inferred within the statistical error.

In Section IV C, we have suggested an explanation for the fact that unfolded sequences of levels without long-range rigidity significantly overestimate the chaoticity parameter f while unfolded sequences of levels that do obey the long-range order of GOE spectra yield correct estimates of f .

To obtain the present results, we have used the one-parameter conditional distribution of Section III A in order to interpolate between regular and chaotic systems. Other models of the NNS distribution — which we could have used as well — are expected to lead to similar conclusions because (i) the Bayesian method is by definition free from binning the observable and (ii) the explanation in Section IV C is independent of the specific conditional

distribution of Section III A.

Our results provide a justification for previous analyses of atomic, molecular, and nuclear level statistics where similar composite spectra were considered. We have in mind the analyses of NNS distributions of experimental nuclear spectra in the ground-state domain carried out, for instance, in Refs. [1, 2, 3, 4, 5, 6, 7, 8, 9, 40], and the analyses of composite spectra in atoms [10, 11, 12] and molecules [13, 14, 15]. Most of these analyses in nuclear systems involve composite ensembles that combine levels from different nuclei. Even in the few cases where the levels under investigation are taken from a single nucleus, levels of different spin or parity are combined to obtain reliable statistics.

Acknowledgement

The authors thank Professor J. Hüfner for useful discussions. They thank Prof. A. Richter and Dr. C. Dembowski for communicating the data used to generate the GOE ensembles. A.Y.A.-M. and M.H.S. acknowledge the financial support granted by Internationales Büro, Forschungszentrum Jülich, that permitted their stay at the Max-Planck-Institut für Kernphysik, Heidelberg.

APPENDIX A: LEVEL SPACING DISTRIBUTION FOR COMPOSITE SPECTRA

Rosenzweig and Porter [10] considered a spectrum S which can be represented as a superposition of m independent sub-spectra S_j each having fractional level density f_j , with $j = 1 \dots m$, and with $0 < f_j \leq 1$ and $\sum_{j=1}^m f_j = 1$. Let $p_j(s)$ denote the NNS distribution for the sub-spectrum S_j with $j = 1 \dots m$ and $p(s)$ the NNS distribution of the spectrum S . We define the associated gap functions

$$E_j(s) = \int_s^\infty ds' \int_{s'}^\infty p_j(x) dx \quad (\text{A1})$$

for the sub-spectra and

$$E(s) = \int_s^\infty ds' \int_{s'}^\infty p(x) dx \quad (\text{A2})$$

for the spectrum S . Mehta [18] has shown that

$$E(s) = \prod_{j=1}^m E_j(f_j s) . \quad (\text{A3})$$

Given $E(s)$, one can find $p(s)$ by taking the second derivative of $E(s)$. The derivation of the exact expression for $p(s)$ can be found in Appendix A.2, p. 402, of Ref. [18]. We aim at an approximate evaluation of $E(s)$ and, thence, of $p(s)$.

We write the cumulative spacing distribution

$$W(s) = 1 - \frac{dE(s)}{ds} \quad (\text{A4})$$

in the form

$$W(s) = 1 + \exp \{ \theta(s) + \ln [-d\theta(s)/ds] \} , \quad (\text{A5})$$

where

$$\theta(s) = \sum_{j=1}^m \ln [E_j(f_j s)] . \quad (\text{A6})$$

In Refs. [33], a simple expression for $W(s)$ was obtained by expanding the exponent in Eq. (A5) in powers of s and neglecting terms of higher order than the second. This procedure was motivated by the fact that $p(s)$ is mainly determined by short-range level correlations. We follow this procedure and obtain

$$W(s) = 1 - \exp \left(-qs - \frac{\pi}{4} Qs^2 \right) , \quad (\text{A7})$$

where

$$q = 1 - \sum_{j=1}^m f_j^2 [1 - p_j(0)] \quad (\text{A8})$$

and

$$Q = \frac{2}{\pi} \left(\sum_{j=1}^m f_j^2 [1 - p_j(0)] + \left\{ \sum_{j=1}^m f_j^2 [1 - p_j(0)] \right\}^2 - \sum_{j=1}^m f_j^3 [2 - 3p_j(0) - p_j'(0)] \right). \quad (\text{A9})$$

The Wigner surmise for each of the p_j 's implies $p_j(0) = 0$ and $p_j'(0) = \pi/2$. The parameter q — given by Eq. (A8) — becomes

$$q = 1 - f, \quad (\text{A10})$$

where

$$f = \sum_{j=1}^m f_j^2. \quad (\text{A11})$$

Since $\sum_j f_j = 1$, we cannot use the mean value of the f_j 's as a measure of the mean fractional density. The parameter f with $0 < f \leq 1$ defined in (A11) is the next-best choice. We refer to f as to the mean fractional level density for the superimposed sequences. The parameter Q is, in principle, given by Eq. (A9). We will, however, replace that expression by another one which we construct as follows.

The NNS distribution is obtained by differentiating the approximate expression (A7) with respect to s ,

$$p(s) = \frac{dW(s)}{ds}. \quad (\text{A12})$$

In going from Eq. (A5) to Eq. (A7), we have neglected higher powers of s in the expansion of $\ln[1 - W(s)]$. This neglect entails, however, that the distribution (A7) does not satisfy the condition of unit mean spacing

$$\int_0^\infty xp(x)dx = \int_0^\infty [1 - W(x)] dx = 1. \quad (\text{A13})$$

In order to satisfy this condition we determine the parameter Q from Eq. (A13) while keeping Eq. (A10) for the parameter q . We do so in order to maintain the correct behavior of a collection of independent GOE subsequences at small values of s . Hopefully, this approximation will take into account some of the effects of the neglected terms in the power-series expansion of the logarithm. The proposed NNS distribution of the composite spectrum

is then given by

$$p(s, f) = \left[1 - f + Q(f) \frac{\pi s}{2} \right] \exp \left[- (1 - f) s - Q(f) \frac{\pi s^2}{4} \right], \quad (\text{A14})$$

where $Q(f)$ is defined by the condition (A13). This procedure yields an implicit relation between Q and f which involves a complementary error function. We have numerically solved the implicit equation and obtained $Q(f)$ for f in the interval of $0.1 \leq f \leq 0.9$. The resulting solution was approximated by the parabolic relation

$$Q(f) = f (0.7 + 0.3f). \quad (\text{A15})$$

With this approximation, the mean spacing differs from unity by less than 0.5%. The distribution (3) coincides with the exact expression up to the 6th decimal digit. The exact values were obtained by doubly differentiating Eq. (A3), see Ref. [18].

APPENDIX B: DETAILS ON THE POSTERIOR DISTRIBUTION

The prior distribution Eq. (7) was evaluated numerically after inserting Eq. (4) into Eq. (7). The result was approximated by the sixth-order polynomial

$$\begin{aligned} \mu(f) = & 1.975 - 10.07f + 48.96f^2 - 135.6f^3 \\ & + 205.6f^4 - 158.6f^5 + 48.63f^6. \end{aligned} \quad (\text{B1})$$

The distribution $p(\mathbf{s}|f)$ assumes very small values even for only moderately large values of N . Therefore, the accurate calculation of the posterior distribution requires some care. In order to simplify the calculation, we have rewritten Eq. (4) in the form

$$p(\mathbf{s}|f) = e^{-N\phi(f)}, \quad (\text{B2})$$

where

$$\begin{aligned} \phi(f) = & (1 - f)\langle s \rangle + \frac{\pi}{4} f (0.7 + 0.3f) \langle s^2 \rangle \\ & - \langle \ln \left[1 - f + \frac{\pi}{2} f (0.7 + 0.3f) s \right] \rangle. \end{aligned} \quad (\text{B3})$$

Here, the notation

$$\langle x \rangle = \frac{1}{N} \sum_{i=1}^N x_i \quad (\text{B4})$$

has been used. We find that the function $\phi(f)$ has a pronounced absolute minimum, say at $f = f_0$. This minimum provides the maximum of the posterior distribution P which is of interest in the neighborhood of f_0 . There one can represent P by parameterizing ϕ in the form of a third-order polynomial,

$$\phi(f) = A + B(f - f_0)^2 + C(f - f_0)^3 . \quad (\text{B5})$$

The parameters A, B, C and f_0 are implicitly defined by Eq. (B3).

In the analysis of the NNS distributions for the coupled microwave resonators [17], the number of spacings for each coupling was so large ($N \simeq 1500$) that a Gaussian distribution

$$P_G(f | \mathbf{s}) \propto \exp\{-NB(f - f_0)^2\} \quad (\text{B6})$$

was found to describe the f -dependence of the posterior $P(f | \mathbf{s})$ very well. Indeed, for a sufficiently large number N of data the posterior should approach a Gaussian. Although this is not a consequence of the Central Limit Theorem, the proof of this statement is similar. Therefore, the posterior distributions obtained in that analysis were Gaussians characterized by a mean value f_0 and the variance $\sigma_0 = 1/\sqrt{2NB}$. The present analysis, however, addresses NNS distributions that involve a considerably smaller number of spacings. Therefore, we cannot further simplify the approximation (B5) and arrive at

$$P(f | \mathbf{s}) = c \mu(f) \exp\left(-N \left[B(f - f_0)^2 + C(f - f_0)^3\right]\right), \quad 0 \leq f \leq 1. \quad (\text{B7})$$

Here, $c = e^{-NA}/M(\mathbf{s})$ is the new normalization constant.

APPENDIX C: INTEGRATION OVER AN UNINTERESTING PARAMETER

We expand on the integration over uninteresting parameters briefly discussed in Subsection IV C. Let the model $p(x|\xi)$ be conditioned by two parameters,

$$\xi = \begin{pmatrix} \xi_1 \\ \xi_2 \end{pmatrix}. \quad (\text{C1})$$

Only ξ_1 is interesting. The precision with which one can infer the value of ξ_1 depends on one's knowledge of ξ_2 . We distinguish two cases of prior knowledge: (i) ξ_2 is known to have the value α and (ii) ξ_2 is unknown. In the first case, $\xi_2 = \alpha$ is simply inserted into the model

so that ξ_1 is inferred from $p(x|\xi_1; \xi_2 = \alpha)$. In the second case, ξ_1 is inferred after ξ_2 has been integrated over. The precision with which ξ_1 can be obtained, is better in the first case than in the second.

As an example we consider the Gaussian model

$$p(x|\xi) \propto \exp\left(-(x - \xi)^T (2C)^{-1} (x - \xi)\right). \quad (\text{C2})$$

Here, the data x form a 2-dimensional vector

$$x = \begin{pmatrix} x_1 \\ x_2 \end{pmatrix} \quad (\text{C3})$$

as do the parameters ξ . The 2-dimensional correlation matrix C contains the variances C_{11}, C_{22} and the correlation coefficient C_{12} . (This model has also been discussed in Chap. 12.2.2 of [38]).

(i) When ξ_2 is known to have the value α , one obtains the Gaussian model

$$p(x|\xi_1; \xi_2 = \alpha) \propto \exp\left(-\left((2C)^{-1}\right)_{11} \left[(x_1 - \xi_1 + (x_2 - \alpha)C_{12}^{-1}/C_{11}^{-1})^2\right]\right) \quad (\text{C4})$$

conditioned by ξ_1 . The posterior distribution of ξ_1 is Gaussian with variance

$$\begin{aligned} \left((C^{-1})_{11}\right)^{-1} &= \left(\frac{C_{22}}{\det C}\right)^{-1} \\ &= C_{11} - C_{12}^2/C_{22}. \end{aligned} \quad (\text{C5})$$

(ii) Integration of Eq. (C2) over ξ_2 yields the Gaussian model

$$\begin{aligned} q(x|\xi_1) &= \int d\xi_2 p(x|\xi_1, \xi_2) \\ &\propto \exp\left(-(2C_{11})^{-1}(x_1 - \xi_1)^2\right) \end{aligned} \quad (\text{C6})$$

conditioned by ξ_1 . The posterior distribution of ξ_1 is Gaussian with variance C_{11} .

The variance (C_{11}) of the second case is larger than the variance (C5) of the first case. The variances agree if the correlation C_{12} vanishes. Then the problem factorises with respect to the parameters ξ_1 and ξ_2 .

[1] A. Y. Abul-Magd and H. A. Weidenmüller, Phys. Lett. B 162, 223 (1985).

- [2] T. von Egidy, A. N. Behkami, and H. H. Schmidt, Nucl. Phys. A 454, 109 (1986); Nucl. Phys. A 481, 189 (1988).
- [3] G. E. Mitchell, E. G. Bilpuch, P. M. Endt, and J. F. Shriner, Jr., Phys. Rev. Lett. 61, 1473 (1988).
- [4] S. Raman, T. A. Walkiewicz, S. Kahane, E. T. Turney, J. Sa, Z. Gàcvzi, J. Wei, K. Allaart, G. Bonsignori, and J. F. Shriner, Jr., Phys. Rev. C 43, 521 (1991).
- [5] J. F. Shriner, Jr., E. G. Bilpuch, P. M. Endt and G. E. Mitchell, Z. Phys. A 335, 393 (1990).
- [6] A. Y. Abul-Magd and M. H. Simbel, J. Phys. G 22, 1043 (1996); 24, 576 (1998).
- [7] J. D. Garrett, J. Q. Robinson, A. J. Foglia, and H.-Q. Jin, Phys. Lett. B 392, 24 (1997).
- [8] J. Enders, T. Guhr, N. Huxel, P. von Neumann-Cosel, C. Rangacharyulu, and A. Richter, Phys. Lett. B 486, 273 (2000).
- [9] J. F. Shriner, C. A. Grossmann, and G. E. Mitchell, Phys. Rev. C 62, 054305 (2000).
- [10] N. Rosenzweig and C. E. Porter, Phys. Rev. 120, 1698 (1960).
- [11] H. S. Camarda and P. D. Georgopoulos, Phys. Rev. Lett. 50, 492 (1983).
- [12] V. V. Flambaum, A. A. Gribakina, G. F. Gribakin, and M. G. Kozlov, Phys. Rev. A. 50, 267 (1994).
- [13] E. Haller, H. Köppel, and L. S. Cederbaum, Chem. Phys. Lett. 101, 215 (1983).
- [14] T. Zimmermann, H. Köppel, and L. S. Cederbaum, J. Chem. Phys. 91, 3934 (1989).
- [15] D. M. Leitner, H. Köppel, and L. S. Cederbaum, J. Chem. Phys. 104, 434 (1996).
- [16] C. I. Barbosa and H. L. Harney, Phys. Rev. E 62, 1897 (2000).
- [17] A. Y. Abul-Magd, C. Dembowski, H. L. Harney, and M. H. Simbel, Phys. Rev. E 65, 056221 (2002).
- [18] M. L. Mehta, Random Matrices, 2nd Edition, (Academic, New York, 1991).
- [19] E. P. Wigner, Oak Ridge National Laboratory Report No. ORNL-2309, 1957.
- [20] O. Bohigas, M.-J. Giannoni, and C. Schmit, Phys. Rev. Lett. 52, 1 (1984).
- [21] T. Guhr, A. Müller-Groeling, and H. A. Weidenmüller, Phys. Rep. 299, 189 (1998).
- [22] Y. Alhassid, Rev. Mod. Phys. 72, 895 (2000).
- [23] F. M. Izrailev, Phys. Rep. 196, 299 (1990).
- [24] A. Y. Abul-Magd, J. Phys. A 29, 1 (1996).
- [25] T. Prosen and M. Robnik, J. Phys. A 26, 1105 (1993); 27, 8059 (1994).
- [26] P. R. Richens and M. V. Perry, Physica D 2, 495 (1998).

- [27] D. Biswas and S. R. Jain, *Phys. Rev. A* 42, 3170 (1990).
- [28] G. Date, S. R. Jain, and M. V. N. Murthy, *Phys. Rev. E* 51, 198 (1995).
- [29] H. L. Harney, A. Richter, and H. A. Weidenmüller, *Rev. Mod. Phys.* 58, 607 (1986).
- [30] C. Ellegaard, T. Guhr, K. Lindemann, J. Nygård, and M. Oxborrow, *Phys. Rev. Lett.* 77, 4918 (1995).
- [31] H. Alt, C. Barbosa, H.-D. Gräf, T. Guhr, H. L. Harney, R. Hofferbert, H. Rehfeld, and A. Richter, *Phys. Rev. Lett.* 81, 4847 (1998).
- [32] A. Abd El-Hady , A. Y. Abul-Magd and M. H. Simbel, *J. Phys. A* 35, 2361 (2002).
- [33] A. Y. Abul-Magd and M. H. Simbel, *Phys. Rev. E* 54, 3292 (1996); *Phys. Rev. C* 54, 1675 (1996).
- [34] T. A. Brody, *Lett. Nuovo Cim.* 7, 482 (1973).
- [35] E. B. Bogomolny, U. Gerland, and C. Schmit, *Phys. Rev. E* 59, R1315 (1999).
- [36] H. Jeffreys, *Proc. of the Roy. Soc. A* 186, 453 (1946); *H. Jeffreys Theory of Probability*, 3rd Edition, Oxford University Press, Oxford 1961.
- [37] R. E. Kass, PhD thesis “The Riemannian structure of model spaces: A geometric approach to inference”, University of Chicago, 1980; R. E. Kass and E. Wassermann, *J. Am. Statist. Assoc.* 91, 1343 (1996).
- [38] H.L. Harney, “Bayesian Inference — Parameter estimation and decisions” Springer Verlag, Heidelberg, 2003.
- [39] T. H. Seligman and J. J. M. Verbaarschot, *J. Phys. A* 18, 2227 (1985).
- [40] A. Abul-Magd, H. L. Harney, M. H. Simbel, and H. A. Weidenmüller, *Phys. Lett. B* 579, 278 (2004).